Master Thesis
Jan Grzegorzewski

Reaction-Diffusion Dynamics With Fractional Brownian Motion

Winter term: 2016

Contents

List of Figures

Motivation

Anomalous diffusion can be observed in many different areas of nature, in particular, related to heterogeneous media like porous rocks, random resistor networks and crowded biological media with its prominent phenomena macromolecular crowding, confinement and macromolecular adsorption [11]. These environments exhibit remarkable characteristics like anomalous diffusion with its most popular power-law behaviour of the Mean-Square-Displacement ($MSD \propto t^{\alpha}$) [5], which violates the Einstein formula $MSD = 2dDt$ and thereby the central limit theorem. Various theoretical models try to encounter anomalous diffusion. One of these models is fractional Brownian motion (fBm). It is modelling a stochastic process with strong correlations of the incerements. FBm was first introduced as family of Gaussian random function by Mandelbrot and Van Ness in 1968 and motivated by examples in economics [9]. In contrast to different models of anomalous diffusion, the fBm approach is plainly phenomenological defined by a power-law of the MSD and thus perfectly qualifies as a starting point to study effects resulting from a power-law MSD.
This thesis focuses on the impact of fBm on enzymatic reactions. Pionier work by Leonor Michaelis and Maud Menten [10] simplified the enzymatic reaction sceme for a concentration based model. As one of the best known and important models of enzyme kinetecs it is of great intereset to study effects on Michaelis-Menten like reactions by fBm. For this purpose a particle based simulation with a fBm integrator of a Michaelis-Menten like reactions was set up. Spatial and temporal effects induced by fBm were studied.
The thesis is organized in four chapters: 1. Fractional Brownian Motion ,2. Particle Based Reaction Diffusion, 3. An Enzyme Reaction With Fractional Brownian Motion and 4. Summary. The first chapter sets up theoretical fondations for fBm. Subsequently, fBm generating algorithms are studied. The second chapter deales with models describing reactions in general but focuses on particle based reaction diffusion. A particle based Reaction Diffusion software RevReaDDy, which dealed as a starting point for the implementation is introduced. Chapter 3 focuses more specifically on enzyme reactions. Followed by a enzymatic simulation model set up with RevReaDDy. Finally results from the simulation are discussed and related to existing literature. Chapter 4 summarizes the content of the thesis.

1 Fractional Brownian Motion

1.1 Introduciton

Wiener process is a continous-time stochastic processes. It is applied to finance, biology, physics and many more because of no or only week correlations of the underlying processes. Brownian motion is the random motion of particles suspended in a fluid, which is modeled by a wiener process. Fractional Brownian Motion (fBm) is a more general family of Gaussian random function then standard Brownian motion with long-range correlations as its defining property. The main objective of this chapter is to explore the theoretical foundation for fBm starting with Brownian motion in the following section. Further algorithms generating fBm are introduced and analyzed in terms of accuracy and performance.

1.2 Brownian Motion

Standard Brownian Motion is a very important and good studied stochastic process. It describes the erratic motion of mesoscopic particles, which first were documented by Jan Ingenhousz in 1785, in particular for coal dust on the surface of alcohol [5]. Later on, in 1827 Robert Brown observed the erratic motion of pollen grains. Brownian Motion has a Gaussian propagator, which has its origin in the Central Limit Theorem (CLT) for a sum of independent and identically distributed random variables.

Definition 1 *Let's assume a set of N independent variables $\{X_i\}$ with a finite variance $\sigma_i^2 = \langle X_i^2 \rangle$ and the mean $\langle X_i \rangle = 0$. The definition of another random variable Y is given by:*

$$Y = \frac{1}{\sqrt{N}} \sum_{j=1}^{N} X_j \tag{1.1}$$

This scenario in which a random variable is defined by the sum of another can be observed generically in nature. The seemingly innocent assumption of independence for the random variable $\{X_i\}$ in the summation results in a Gaussian distribution $\rho(y)$ in the limit of large N with $\rho(y)dy = P(y < Y < y + dy)$

$$\rho(y) = \frac{1}{\sqrt{2\pi}\sigma} e^{-\frac{y^2}{2\sigma^2}} \tag{1.2}$$

A calculation of this very interesting result can be found in the appendix 5.1. Microscopic processes with independent random position changes of a particle, thus

have a Gaussian distribution function for the overall change in position. Therefore a random walk converges toward the Wiener process.
With Bayes' theorem and an initial delta-distribution one can show that transition probability $T_t(y|0) = \rho_t(y)$ is equivalent to the particle density distribution. One can find the calculation in the appendix 5.2. The above-mentioned elaborations motivate the reason for a process with a Gaussian transition probability. A processes with Gaussian distributed transition probability and uncorrelated increments is called Wiener process (Standard Brownian motion).

Definition 2 *Brownian motion described by the Wiener process is a stochastic process* $\{W_t\}_{t\geq 0} : \Omega \to \mathbb{R}^d$ *with* $W_t(\omega)$ *being the position of a particle with* $\omega \in \Omega$ *at time* $t \in T$ *in the observation time* $T = [0, \infty)$*. It has a fixed* $x \in \mathbb{R}^d$ *as its origin. The transition probabilities are [4]:*

$$T_t(y|x) := (2\pi t)^{-\frac{d}{2}} exp\left(-\frac{||x-y||^2}{2t}\right) \text{ for } y \in \mathbb{R}^d, t > 0 \tag{1.3}$$
$$T_0(y|x) = \delta(x-y)$$

The Wiener process is a Gaussian process with mean $\langle W_t \rangle_y = x$ and particle position $W_o = x$ at $t = 0$. Its variance is $\langle W_t^2 \rangle_y = t$. It has a property called Brownian scaling:

$$\{\hat{W}_t := \frac{1}{c} W_{c^2 t}\}_{t\geq 0} \qquad \text{if } \{W_t\}_{t\geq 0} \tag{1.4}$$

A Wiener process has self-similar and fractal paths as a result from Brownian scaling. However it is a purely mathematical model with missing connection to the strength of diffusion of a particle. Fick's empirical second law describes how diffusion causes the concentration to change over time:

$$\frac{\partial}{\partial t} c(\boldsymbol{r}, t) = -\nabla J(\boldsymbol{r}, t) = D\Delta c(\boldsymbol{r}, t) \qquad \text{with} \qquad \Delta = \nabla^2 \tag{1.5}$$

With Fick's first law $J(\boldsymbol{r}, t) = -\nabla c(\boldsymbol{r}, t)$ and D being the flux of particles and the diffusion coefficient, respectively. Fick's first law is a result from the linear response theory. Fick's second law can be derived from the continuity equation and Fick's first law. The Concentration $c(\boldsymbol{r}, t)$ can be interpreted as a probability distribution, if properly normalized $\int d\boldsymbol{r} c(\boldsymbol{r}, t) = 1$. The transition probability of the Wiener process builds the foundation for a more physical description of a propagator:

$$P(\boldsymbol{r}, t) = \left(\frac{2\pi\delta\boldsymbol{r}^2(t)}{d}\right)^{-\frac{d}{2}} exp\left(-\frac{\boldsymbol{r}^2 d}{2\delta\boldsymbol{r}^2(t)}\right) \tag{1.6}$$

One can show that the propagator is solving the diffusion equation eq. (1.5) with $\delta\boldsymbol{r}^2(t) = 2dDt$ and the meaningful initial condition of vanishing concentration at

boundaries:

$$c(\pm\infty, t) = 0 \tag{1.7}$$

The calculation can be found in the appendix 5.3. Brownian scaling applies as a property also to the propagator of Brownian motion. There exists a scale-free form of the Gaussian propagator as a more intuitive consequence of Brownian scaling.

$$P(\boldsymbol{r}, t) = r^{-d}\mathcal{P}_{gauss}(\hat{\boldsymbol{r}}) \qquad \text{with} \qquad \hat{\boldsymbol{r}} = \frac{\boldsymbol{r}}{\sqrt{2Dt}} \tag{1.8}$$

1.3 Fractional Brownian Motion

In this section the theoretical foundation for continious-time and discrete-time Fractional Brownian Motion will be set. In the previous section the MSD has been shown

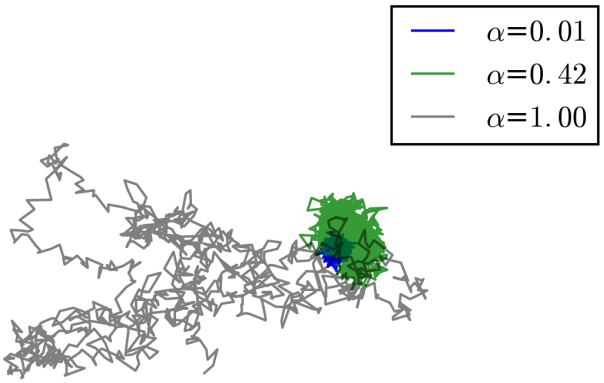

Figure 1.1: shows 3D trajectories of fBm for different α generated with the Lowen algorithm for $K_\alpha = 1$, $\Delta t = 1$ and the trajectory length $M = 1000$.

to be linear with time as a result of the central limit theorem. In normal liquids this behaviour can be seen already at time scales higher than picoseconds [5]. Nevertheless, many experiments show that the MSD has a power law behaviour ($\delta r^2(t) \propto t^\alpha$ for $0 < \alpha < 1$). Thus, the central limit theorem does not hold, not even for long time scales. It can be shown that persistent correlations of the increments are present. In soft matter, like polymers, a subdiffusive behaviour is typically present in a time window but finally the linear MSD takes over. Fractional Brownian motion instead

examines the case that the central limit theorem is violated for all time scales. The basic feature of fBm's is that the "span of interdependence" between their increments can be said to be infinite [9]

Definition 3 *Just like the Wiener process, continous-time Fractional Brownian motion (ctfBm) is a continous-time Gaussian process* $\{B_t^\alpha\}_{t\geq 0} : \Omega \to \mathbb{R}^d$. *Therefore it is fully specified by its mean* $\langle B_t \rangle = 0$ *and its covariance function* $Cov[B_t^\alpha, B_s^\alpha] = \frac{\sigma^2}{2}[t^\alpha - 2(s-t)^\alpha + s^\alpha]$

With the mean and the covariance defined, the mean square displacement can be calculated as:

$$\langle (B_t^\alpha - B_s^\alpha)^2 \rangle = (s-t)^\alpha \sigma^2 \tag{1.9}$$

Lets define another connected random variable: the continous-time fractional Gaussian noise (ctfGn).

Definition 4 *ctfGn is a continous-time Gaussian process* $\{X_t^\alpha\}_{t\geq 0} : \Omega \to \mathbb{R}^d$ *with* $\langle X_t^\alpha \rangle = 0$ *and variance* $Var[X_t^\alpha] = \langle (X_t^\alpha)^2 \rangle = \sigma^2$. *It is the derivative of* B_t^α*:*

$$B_t^\alpha = \int_0^t X_\epsilon^\alpha d\epsilon \tag{1.10}$$

Thus $X_t^\alpha = dB_t^\alpha / dt$ and the covariance function for ctfGn is:

$$Cov[X_t^\alpha, X_s^\alpha] = \frac{d^2 B_t^\alpha B_s^\alpha}{dtds} = -\sigma^2 \frac{d^2 |t-s|^\alpha}{dtds} \tag{1.11}$$

$$= \alpha(\alpha-1)\sigma^2 |t-s|^{\alpha-2} + \alpha\sigma^2 |t-s|^{\alpha-1} \delta(t-s) \tag{1.12}$$

For Wiener white noise ($\alpha = 1$) the first therm (the correlation) disappears:

$$Cov[X_t, X_s] = \sigma^2 \delta(t-s) \tag{1.13}$$

The spectrum density function is defined as the Fourier transform of the autocovariance function:

$$S(\omega) = \int_{-\infty}^{\infty} Cov[X_t, X_0] exp[-2\pi i \omega t] dt \tag{1.14}$$

For algorithmic purpose discrete time fractional Brownian Motion (fGm) and Noise (fGn) are relevant as well:

$$B_t^\alpha = \sum_{i=0}^{k} X_i^\alpha \tag{1.15}$$

The covariance function for fGm is similar to ctfGm but different for fGn in comparison to ctfGn:

$$\begin{aligned} Cov[X_n^\alpha, X_m^\alpha] &= \langle (B_n^\alpha - B_{n-1}^\alpha)(B_m^\alpha - B_{m-1}^\alpha) \rangle \\ &= \frac{\sigma^2}{2}[(n-m-1)^\alpha - 2(n-m)^\alpha + (n-m+1)^\alpha] \end{aligned}$$

and with stationarity:

$$Cov[X_0^\alpha, X_m^\alpha] = \frac{\sigma^2}{2}[(n-1)^\alpha - 2n^\alpha + (n+1)^\alpha] \tag{1.16}$$

A more detailed study on fBm and fGm can be found in [12]. Similar to the argumentation for Brownian motion also fBm need a connection to the strength of diffusion. This connection is introduced by the variance of fGn as:

$$\sigma^2 = 2dK_\alpha \Delta t \tag{1.17}$$

The Mean square displacement for fBm follows from eq. (1.9) as:

$$\delta r^2(t) =< \Delta R(t)^2 >= 2dK_\alpha t^\alpha \tag{1.18}$$

with $K_\alpha > 0$ being the generalized diffusion coefficient. It is not quite the diffusion constant from Fick's law due to different units.
In the following properties of a more physical description of fBm will be discussed:

- The single particle density $\rho(\boldsymbol{r}, t) = \delta(\boldsymbol{r} - \boldsymbol{R}(t))$ describes the density of a particle, which is localized at position $\boldsymbol{R}(t)$. Its correlation function $P(\boldsymbol{r} - \boldsymbol{r}', t - t') = V\langle \rho(\boldsymbol{r}, t)\rho(\boldsymbol{r}', t') \rangle$ is also called Van Hove self-correlation function (in this context the propagator). V refers to the volume. From now on we will consider an isotropic system $r = |\boldsymbol{r}|$. As for Brownian motion with independent increments the correlated increments $\Delta R(t)$ of fractional Brownian motion are assumed to follow a Gaussian distribution with zero mean. Thus the correlation function of the single particle density results in:

$$P(r, t) = [2\pi\delta r^2(t)/d]^{-\frac{d}{2}} e^{\frac{-r^2 d}{2\delta r^2(t)}} \tag{1.19}$$

- The propagator of fBm can be transformed into a scale free form. It is related to the scale free from of standard Brownian motion eq. (1.8):

$$P(\boldsymbol{r}, t) = \boldsymbol{r}^{-d} \mathcal{P}_{gauss}(\hat{\boldsymbol{r}}) \qquad \text{with} \qquad \hat{\boldsymbol{r}} = \frac{\boldsymbol{r}}{\sqrt{2K_\alpha t^\alpha}} \tag{1.20}$$

- The van hove correlation function can be transformed via the spatial Fourier transform into its wave-number representation, which is called the self-intermediate

scattering function. Again for isotropic systems one can write $|\boldsymbol{k}| = k$.

$$F_s(k,t) = \langle \rho(k,t)\rho(k',t')\rangle = \int d^d r e^{-ikr} P(r,t) \tag{1.21}$$

$$= \langle e^{-ik\Delta R(t)} \rangle \tag{1.22}$$

- The intermediate scattering function for the single particle density turns out to be the characteristic or moment generating function of $\Delta R(t)$ by expanding it for small wavenumbers $k \to 0$ one can get the moments. Its logarithm returns the cumulants. For Gaussian propagators with zero-mean all but the second cumulants vanish. For non-Gaussian transport also further cumulants are non-zero. Therefore, it is used to indicate beyond Gaussian transport. The non-Gaussian parameter is defined as:

$$\alpha_2 = \frac{d\delta r^4(t)}{(d+2)[\delta r^2(t)]} - 1 \tag{1.23}$$

- An other important quantity is the dynamical structure factor, which is the time-frequency Fourier transform of the intermediate scattering function:

$$F_s(k,z) = \langle \rho(k,z)\rho(k',z')\rangle = \int_0^\infty dt e^{-itz} P(k,t) \text{ for } k \to 0, \mathrm{Im}(z) > 0 \tag{1.24}$$

$$= \frac{1}{-iz} - \frac{k^2}{2d}\int_0^\infty dt e^{izt} \delta r^2(t) + \mathcal{O}(k^2) \tag{1.25}$$

For the velocities as our random variables $\partial_t \boldsymbol{R}(t) = \boldsymbol{\xi}(t)$ also the Velocity auto correlation function is of interest. Velocities correspond to continuous-time fractional Gaussian noise in the mathematical description.

- Velocities can be used to calculated the Velocity Autocorrelation Function (VACF):

$$Z(|t-t'|) = \frac{1}{d}\langle \boldsymbol{\xi}(t)\boldsymbol{\xi}(t')\rangle = \frac{1}{2d}\frac{d^2}{dt^2}\delta r^2(t-t') \tag{1.26}$$

The VACF in the frequency domain for fBm is:

$$\tilde{Z}(z) \overset{\mathrm{Im}(z)>0}{=} K_\alpha \Gamma(1+\alpha)(iz)^{1-\alpha} \tag{1.27}$$

The calculation can be found in the appendix 5.4

1.3.1 Algorithm

The algorithm of choice will be needed as the integrator of motion in a particle based reaction-diffusion software with preferably long trajectories. Therefore exactness

and performance of the algorithm matter. In literature several algorithms were studied. Promising exact methods are: Cholesky [15], Hosking [7], Davis-Harte [15] and Lowen [8] method. Cholesky method claim to perform $\mathcal{O}(M^3)$ in respect to the length of trajectory M and even $\mathcal{O}(M^2)$ for every next trajectory. Davis-Harte and Lowen method claim to be exact and fast $\mathcal{O}(Mlog(M))$ [3][8]. There are further algorithms with even faster performance (e.g. the $RMD_{3,3}$- method [15] with $\mathcal{O}(M)$) . However, they are approximations. In order to choose an algorithm. Three algorithms were analyzed in terms of accuracy and speed. 1.Cholesky 2.Lowen and 3. Our own algorithm.

Cholesky Method

(cite the thesis of Ton Dieker) $\mathcal{O}(M^3)$

Our Algorithms

The VACF in the frequency domain will be used to modify standard Brownian motion velocities, which are easily computable, to generate increments. The starting point are the velocities $\partial_t \boldsymbol{R}(t) = \boldsymbol{\xi}(t)$. The increments can be decomposed in its Fourier modes for real frequencies $z = \omega$:

$$\tilde{\boldsymbol{\xi}}_T(\omega) = \int_{-\frac{T}{2}}^{\frac{T}{2}} dt e^{i\omega t} \boldsymbol{\xi}(t) \tag{1.28}$$

For a finite observation time T the Wiener-Khinchin theorem applies :

$$\lim_{T\to\infty} \frac{1}{T} \langle |\tilde{\boldsymbol{\xi}}_T(\omega)|^2 \rangle = 2\,\mathrm{Re}\left(\tilde{Z}(\omega)\right) \tag{1.29}$$

For white noise one gets:

$$\lim_{T\to\infty} \frac{1}{T} \langle |\tilde{\boldsymbol{\eta}}_T(\omega)|^2 \rangle = const. \tag{1.30}$$

Fractional correlations can be incorporated via its VACF:

$$\tilde{\boldsymbol{\xi}}(\omega) = \sqrt{2\,\mathrm{Re}\left(\tilde{Z(\omega)}\right)}\tilde{\boldsymbol{\eta}}(\omega) \tag{1.31}$$

With $\tilde{\boldsymbol{\xi}}(\omega)$ being fractional Brownian velocities in the frequency domain. Its Fourier-back-transform results in fractional Brownian velocities in the time domain.

$$\boldsymbol{\xi}(t) = \int d\omega e^{i\omega t} \tilde{\boldsymbol{\xi}}(\omega) \tag{1.32}$$

In the following an algorithm, which generates fractional Brownian noise will be introduced. The algorithm is based on the Davis-Harte algorithm [2]. The idea is to use the calculated VACF and thereby modify conventionally generated Gaussian

random variables. All the increments should be generated beforehand. With this concept it is difficult to include forces. For computational reasons the pervious elaborations on how to generate fractional Brownian increments have to be transformed into a discrete form, thereby the solution is no longer exact, which will be shown in the analysis part of the algorithm.

$$\boldsymbol{\eta}(t) \longrightarrow \boldsymbol{\eta}_j(t) \text{ with } j = 0, 1, 2, ..., n \text{ , } n = \text{amount of steps} \tag{1.33}$$

For a n-steps long trajectory one can write:

$$\Delta \boldsymbol{R}_n(t) = \sum_{j=0}^{n} \boldsymbol{\eta}_j \Delta t \tag{1.34}$$

The following algorithm is explained for one dimension and can be easily extended for more dimensions. The MSD can be written as:

$$< \Delta R_j(t) >= 2K_\alpha(\Delta t j)^\alpha \tag{1.35}$$

The algorithm goes as follows:

1. M independent normally distributed random increments are generated:

$$\eta_k(t) = \mathcal{N}(0, \sqrt{\Delta t}) \text{ with } k = 0, 1, 2, ..., M \tag{1.36}$$

   $M > n$ more increments are generated to counteract the boundary problem in the discrete Fourier transform, which is shown in fig. 1.2(a) and fig. 1.2(b)

2. Via discrete Fourier transform these increments are transformed into the frequency domain:

$$\tilde{\eta}_l(z) = \sum_{k=0}^{M-1} \eta_k e^{\frac{-i2\pi lk}{M}} \Delta t \text{ with } l = 0, 1, 2, ..., M \tag{1.37}$$

$$\tag{1.38}$$

   By comparison with the eq. (1.28) one can see that:

$$z \to l\Delta z \text{ , } \Delta z = \frac{2\pi}{M\Delta t} \text{ , } t \to j\Delta t \text{ and } \int dt \to \sum \Delta t \tag{1.39}$$

3. Comparable to eq. (1.31) correlations are incorporated:

$$\tilde{\xi}_l(z) = \tilde{\eta}_l(z)\sqrt{2Re(\tilde{Z}_l(z))} \tag{1.40}$$

   with $\tilde{Z}(z) \to \tilde{Z}_l(z)$ as introduced in eq. (1.39):

$$\tilde{Z}_l(z) = K_\alpha\Gamma(1+\alpha)(i2\pi l\Delta z)^{1-\alpha} = K_\alpha\Gamma(1+\alpha)(il\frac{2\pi}{M\Delta t})^{1-\alpha} \tag{1.41}$$

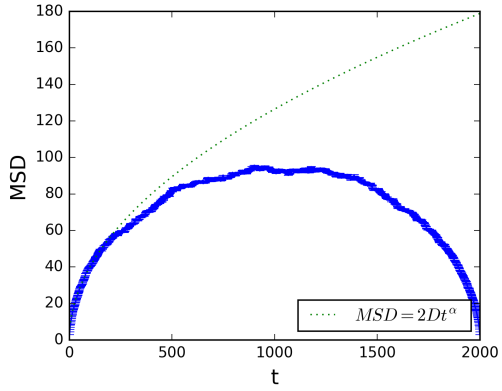

(a) Ensemble MSD without the correction introduced in eq. (1.42)

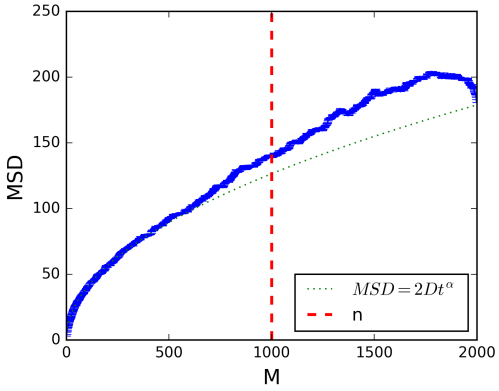

(b) Ensemble MSD with correction introduced in eq. (1.42). The side of the red bar indicates the threshold for the remaining increments for $M = 2n$

4. The discrete Fourier transform has a downside compared to the continuous Fourier transform, as already noted in the beginning of this section. The VACF is zero at zero-frequency $\tilde{Z}_{l=0}(z = 0) = 0$. From eq. (1.40) also the first increment in the frequency domain is zero $\tilde{\xi}_{l=o}(z = 0) = 0$. Due to eq. (1.37) also the following relation holds:

$$\tilde{\xi}_{l=o}(z) = \sum_{k=0}^{M-1} \xi_k e^0 \Delta t = \Delta R_M \tag{1.42}$$

ΔR is the distance between the starting point and the position of the particle. Therefore, the particle would travel after M steps back to its initial position. The effect on the ensemble averaged mean square displacement can be seen in fig. 1.2(a). Instead, the zero-increment in the frequency domain is calculated as follows:

$$\tilde{\xi}_{l=o}(z) = \mathcal{N}(0, \sqrt{2K_\alpha (M\Delta t)^\alpha}) \tag{1.43}$$

This equation would be correct if we assumed fractional Brownian motion to be a Markovian process, which certainly is not the cause. This is also the reason why M have been chosen to be bigger than n. The presumption is, that the impact of the approximation would be negligible with increasing distance to ΔR_M and negligible at ΔR_n. The impact on the ensemble averaged MSD can be seen in fig. 1.2(b). This can be thought of as a finite-time correction.

5. Fractional Brownian increments in the time domain result from the reverse

Fourier transform:

$$\xi_k = \frac{1}{2n} \sum_{l=0}^{2n-1} \tilde{\xi}_l e^{\frac{2\pi i l k}{2n}} \Delta z \tag{1.44}$$

Only n increments are taken into account ξ_j for $j = (0, 1, .., n)$.

The described algorithm can be performed independently for every Cartesian component of the three dimensional fractional Brownian motion. The Cartesian component are not correlated.

Lowen

The previous algorithm had down draws in terms of convergence close to 0 and close to the overall simulation time. therefore a algorithm of Steven B. Lowen [8] had been implemented. Lowens algorithm claims to be both both fast ($\mathcal{O}(NlogN)$) and exact. However our implementation show not to be exact, which can be seen in the analysis part. The algorithm goes as follows:

1. Compute a periodic auto-covariance function of $R_\xi(n)$ of a stochastic process $\xi(n)$:

$$R_\xi(n) = \begin{cases} \frac{1}{2}\left[1 - \left(\frac{n}{N}\right)^\alpha\right] & \text{for } 0 \leq n \leq N \\ R_\xi(2N - n) & \text{for } N \leq n \leq 2N \end{cases} \tag{1.45}$$

2. Transform the auto-covariance function via FFT. The result is called the spectral density of the stochastic process $\xi(n)$:

$$S_\xi(k) = FFT(R_\xi(n)) \tag{1.46}$$

3. Calculate $\tilde{\xi}(k)$ the Fourier transform of the stochastic process $\xi(n)$:

$$\tilde{\xi}(k) = \begin{cases} 0 & \text{for } k = 0 \\ exp(i\theta)\eta\sqrt{S_\xi(k)} & \text{for } 0 \leq k \leq N \\ \eta\sqrt{S_\xi(k)} & \text{for } k = N \\ \tilde{\xi}^*(2N - k) & \text{for } N \leq k \leq 2N \end{cases} \tag{1.47}$$

$\tilde{\xi}^*$ denotes the complex conjugate of $\tilde{\xi}$. θ is a random variable uniformly distributed in $(0, 2\pi]$. η is a random Gaussian variable with zero mean and variance 1 ($\mathcal{N}(0, 1)$).

4. Perform the inverse Fourier transform on $\tilde{\xi}(k)$ and use the first half of the resulting stochastic process $\xi(n)$ multiplied by a factor:

$$\xi(n) = FFT^{-1}(\tilde{\xi}(k)) \tag{1.48}$$

$$B_n^\alpha = \sqrt{2K_\alpha N^\alpha \Delta t^\alpha}(\xi(n) - \xi(0)) \qquad \text{for } 0 \leq n \leq N \tag{1.49}$$

Lets check the resulting auto-covariance function.

$$Cov[B_n^\alpha, B_m^\alpha] = 2K_\alpha \Delta t^\alpha N^\alpha \langle (\xi(n) - \xi(0))((\xi(m) - \xi(0))\rangle \tag{1.50}$$

$$= 2K_\alpha \Delta t^\alpha N^\alpha \langle \xi(n)\xi(m)\rangle - \langle \xi(0)\xi(m)\rangle - \langle \xi(0)\xi(n)\rangle + \langle \xi(0)^2\rangle \tag{1.51}$$

$$= \frac{2K_\alpha \Delta t^\alpha}{2}[n^\alpha - 2(m-n)^\alpha + n^\alpha] \qquad \text{for } n < m \tag{1.52}$$

The auto-covariance function indeed satisfies the condition for fBm with variance similar to eq. (1.17). In step 3 the phase and amplitude of the Fourier transform $\xi(m)$ were chosen to be random as suggested in [14]. The second derivative of $R_\xi(n)$ is positive. $R_\xi(n)$ results in a periodic function with non negative curvature. Its Fourier transform $S_\xi(k)$ is , real, symmetric and non-negative for all k. $S_\xi(k)$ is then a valid power spectral density function of the discrete-time periodic process $\xi(n)$ with period $2n$ and $R_\xi(n)$ its valid auto-covariance function [8]. This algorithm is actually using the property of Brownian scaling eq. (1.4) to generate a realization of fBm with non negative auto-covariance function. The algorithm was implemented in c++ with a 1 dimension Fast Fourier transform from the package FFTW3. FFTW computes an unnormalized DFT. Thus, computing a forward followed by a backward transform results in the original array scaled by the size of the array. The size of the array is $2M$ in Lowens algorithm. Thus a random variable should be divided by $\sqrt{2N}$ to have a normalized FFT.

Accuracy Analysis

The algorithms were implemented in python and c++. For the c++ implementation a wrapper to python was added. All algorithms have been analyzed by an analysis class. The c++ implementation is using FFTW library for the Fast Fourier Transform and Mersenne-Twister (gsl_rng_mt19937) as the random number generator. Python implementations were developed beforehand and only serve as reference. Python uses the numpy.fft library for the Fast Fourier Transform and also the Mersenne-Twister random number generator.

To get insight into stochastic algorithms observables have to by studied. Observables of an stochastic process are generally averaged values. The motivation of choosing fBm was its power law behaviour of the MSD. It is therefore to be reasonable to analyze first this observable. It can be calculated as the ensemble- or time average. A difference in time and ensemble average would show a violation of ergodicity. A comparison for all the three implemented algorithms can be seen in fig. 1.2. All algorithm show good accuracy between ensemble and time averaged MSD, besides for long lag times for the time averaged MSD due to decreasing statistics. Our algorithm tend to result in too small MSDs for small lag times particularly for small α, which is going be shown later on. This is caused by the finite amount of samples in the discrete Fourier transform. In the following figures all MSD plots are ensemble averages. They are computationally cheaper.
Secondly time-reversibility had been checked. FBm should be time reversible as shown in [6]. In fig. 1.3 MSDs for forward time and for backward time were plotted.

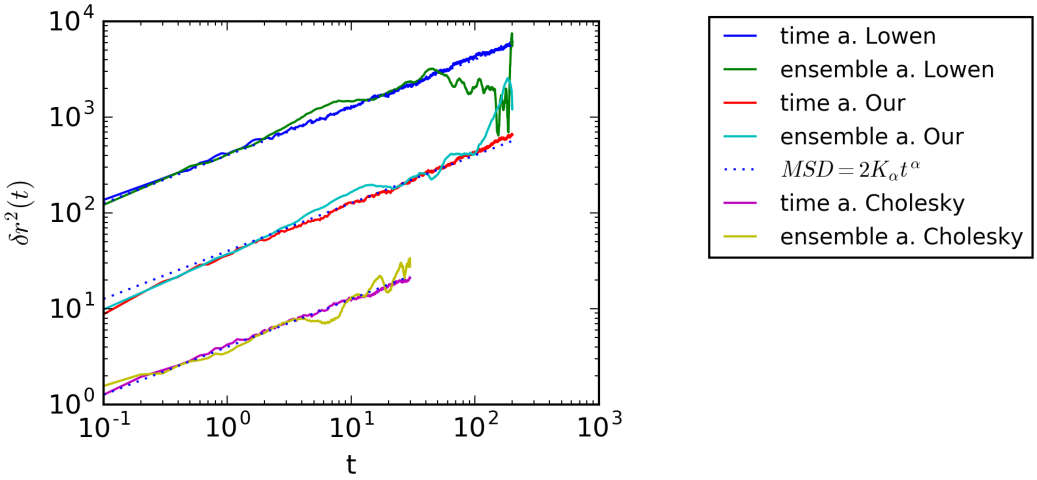

Figure 1.2: Comparison of MSD between time-average, ensemble-average ($N = 1000$) ,$\alpha = 0.5$, $\Delta t = 0.1$ for the three algorithms.
Cholesky: $D = 2$, $M = 300$.
Our $D = 20$ $M = 2000$,
Lowen: $D = 200$ $M = 2000$.

No difference can be seen. α had been chosen to be 0.1. Thereby our algorithm has an even stronger deviation from the desired power law. A strong influence of α on

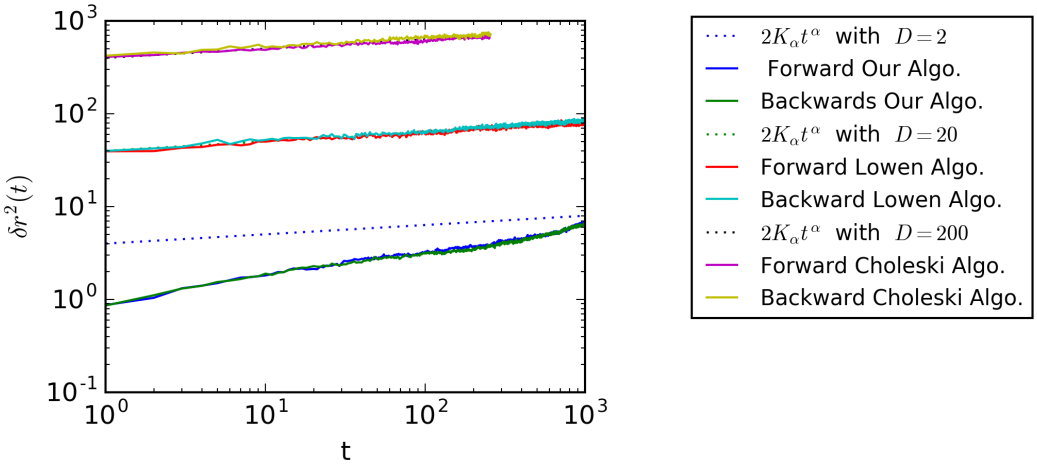

Figure 1.3: The plot show ensemble averaged MSDs for forward time and backward time over $N = 2000$ trajectories for $\alpha = 0.1$, $\Delta t = 0.1$ and trajectory length $M = 1000$ and $K_\alpha = 2$ for Our algorithm, $M = 1000$ $K_\alpha = 20$ for Lowen algorithm and $M = 256$ $K_\alpha = 200$ for Cholesky algorithm.

the accuracy of MSD for our algorithm can be seen. The influence of α on the MSD for the three algorithms are shown in fig. 1.4. In the limit of Brownian motion $\alpha = 1$

the artifacts for small lag-times in the our algorithm vanish. Cholesky and Lowen show no deviation to the expected MSD for all α.

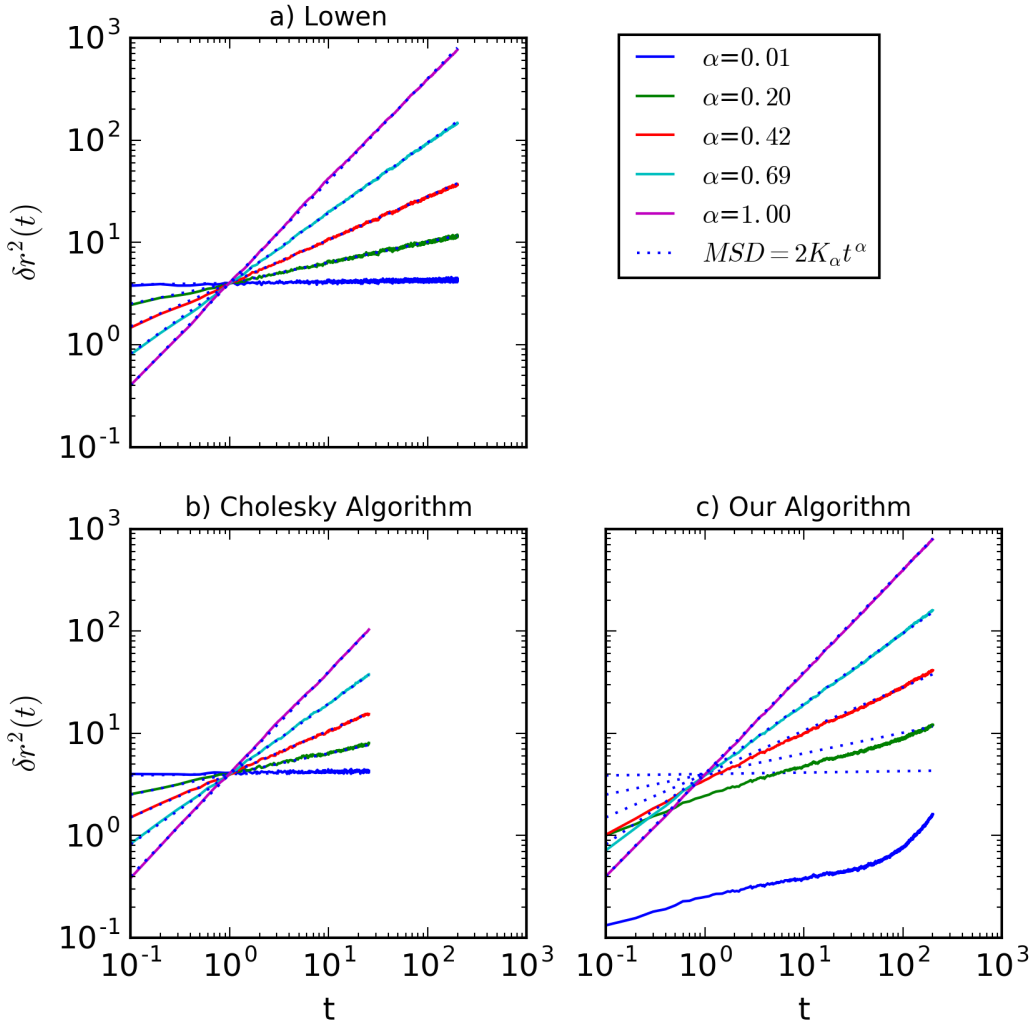

Figure 1.4: All three plots show an ensemble averaged MSD over $N = 2000$ trajectories for $0.1 < \alpha < 1.0$ with $K_\alpha = 2$,$\Delta t = 0.1$ and trajectory length $M = 2000$ for Our and Lowen algorithm, $M = 256$ for Choleski algorithm. a) Our algorithm and b) Lowen algorithm c) Choleski algorithm.

FBms property of self similarity can be used to plot a scale free version of the density distribution. The scale free version was introduced in eq. (1.20). The scaled density distribution is not depended on time but overlaps for all times. In fig. 1.5 histograms over $N = 10000$ single trajectories at various times ($100 \leq t \leq 1000$) were calcualted and rescaled according to eq. (1.20). The dashed line show the expected distribution. For Cholesky and our algorithm no deviations from the analytical line is obvious. For Lowens algorithm systematically small changes to the analytical

value can be observed. However, the distribution of fBm should stay a Gaussian for all times. As introduced in eq. (1.23) the non-Gaussian parameter should be zero. The Non-Gaussian parameter has been plotted for $0 \leq t \leq 1000 (\leq 356$ for Cholesky) $\alpha = 0.5$ in fig. 1.6 a). Our and Cholesky algorithm perform as expected. Lowen however show deviation from a Gaussian distribution increasingly towards the end of the trajectory. In fig. 1.6 b) the influence of α on the non-Gaussian parameter for the Lowen algorithm was tested. For small α the distribution is closer to a Gaussian. In our implementation Lowens algorithm is not exact as claimed in [8].

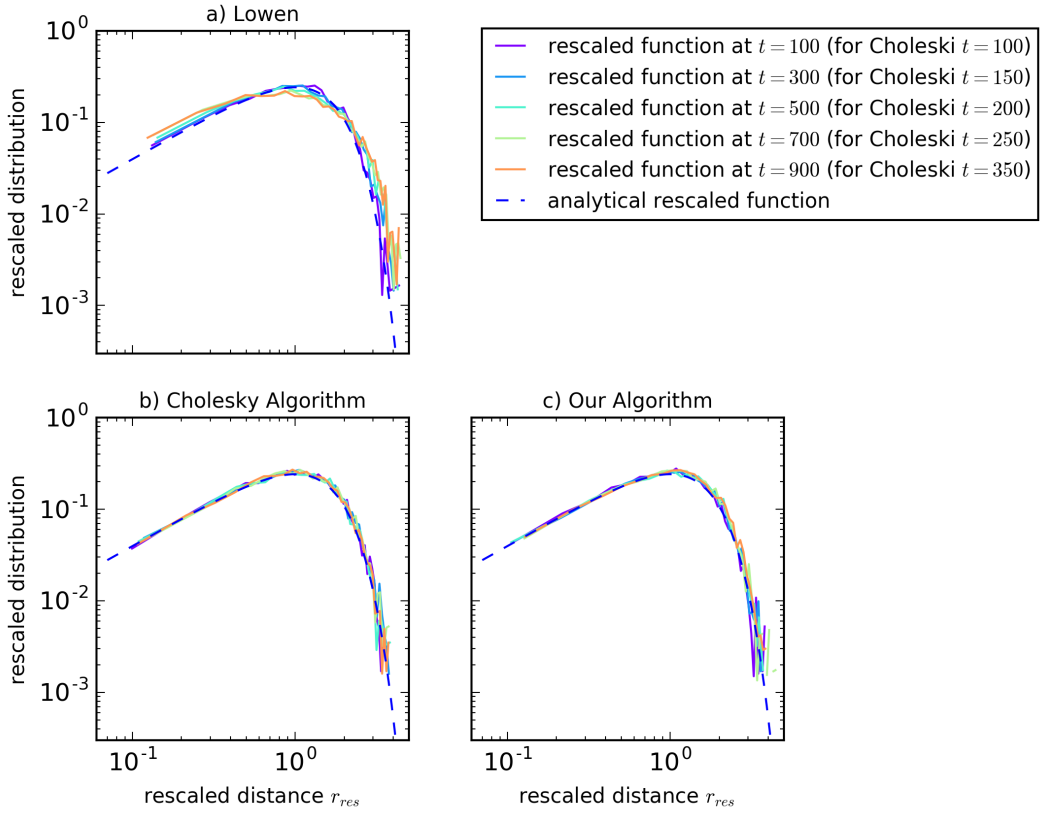

Figure 1.5: All three plots show the scale free form of the propagator at different times as introduced in eq. (1.20) as an histogram over $N = 10000$ trajectories for $\alpha = 0.5$ with $K_\alpha = 2$,$\Delta t = 0.1$ for all three algorithm, at different times $100 < t < 900$

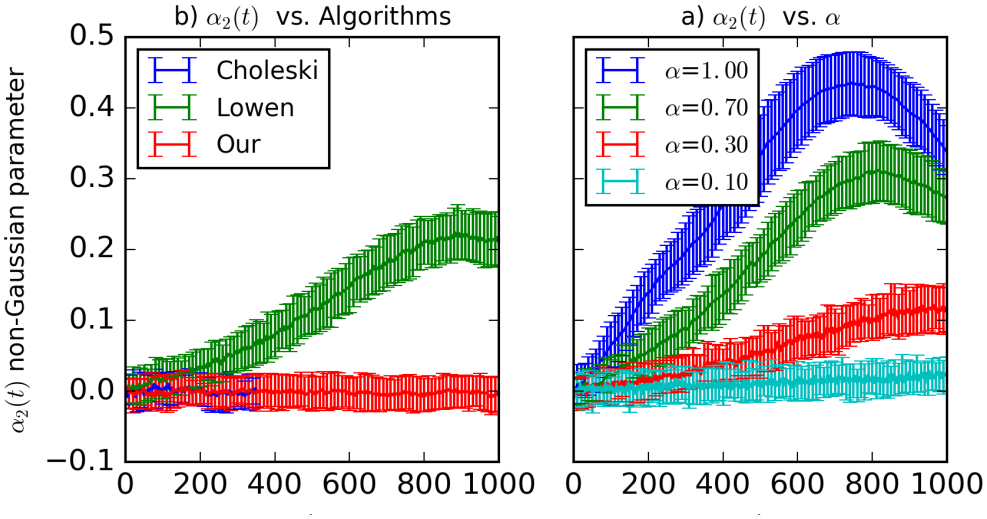

Figure 1.6: a) Non-Gaussian-Parameter as introduced in eq. (1.23) for all three algorithms with $K_\alpha = 2$, $N = 5000$,$\alpha = 0.5$ (Lowen and Our $M = 1001$; Choleski $M = 356$), $\Delta t = 1$ averaged over 50 non-Gaussian-Parameter with its variance displayed as an error bar.
b) Non-Gaussian-Parameter for Lowen algorithms with $K_\alpha = 2$, $N = 5000$, $M = 1001$, $\Delta t = 1$ and for various $0.1 \leq \alpha \leq 1.0$ averaged over 50 non-Gaussian-Parameter with its variance displayed as an error bar.

Performance Analysis

The performance in respected to sample size (trajectory length) and number of samples (amount of trajectories) was analyzed in fig. 1.7 b) . Thereby the most promising, in terms of exactness, Cholesky algorithm scales in respect to the trajectory length M with $\mathcal{O}(M^3)$. Our application of the integrator desire long trajectories. It is not reasonable to use such a slow algorithm. Even if every next trajectory with the same α and length is of $\mathcal{O}(M^2)$ [15]. In fig. 1.7 a) one can see Cholesky to scale slow with the amount of trajectories N. Although one should keep in mind that the trajectory length had to be chosen $M = 128$ compared to $M = 1000$ as for Our and Lowens algorithm to get comparably small values. Lowens and Our algorithm perform both $\mathcal{O}(Mlog(M))$ in respect to the trajectory length as a result of the FFT and $\mathcal{O}(N)$ in respect to the amount of trajectories.

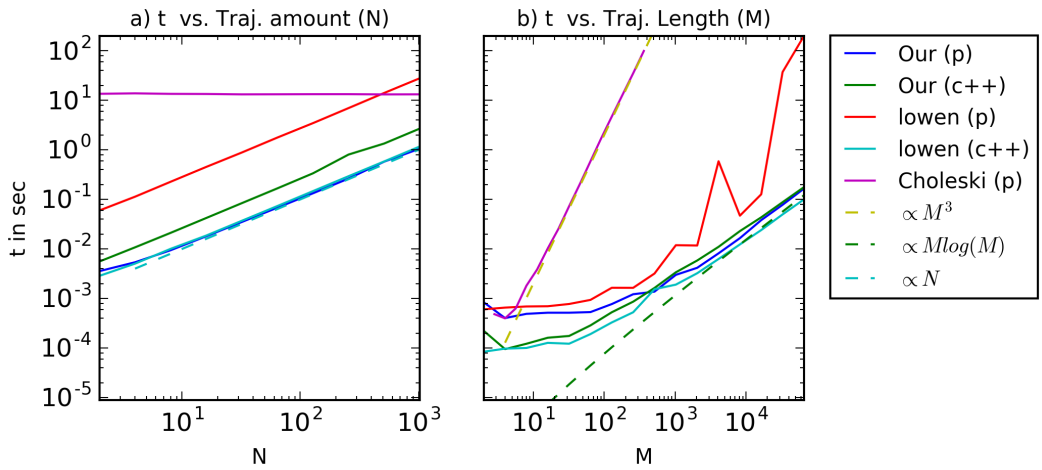

Figure 1.7: a) Algorithmic scaling of computational time in respect to the amount of trajectories N for trajectory length $M = 1000$, ($D = 2$, $\alpha = 0.5$, $\Delta t = 1$) of Lowen and our own algorithm. Both implemented in c++ and python (p). The Cholesky algorithm was implemented in python with $M = 128$.
b) Algorithmic scaling of computational time in respect to the trajectory length M for a single trajectory $N = 1$, ($D = 2$, $\alpha = 0.5$, $\Delta t = 1$). Lowen and our own algorithms are implemented in c++ and python (p). Cholesky is only implemented in python (p).

2 Particle Based Reaction Diffusion

(von franks Vortrag das Bild mit den unterschiedlichen Methoden zur genererieung von Reactiondiffusions systemen). This chapter is going to discuss particle based reaction diffusion. Particle based reaction diffusion is going to be put in relation to different reaction diffusion studying methods. Analytical solutions for resulting ordinary differencial equation exist under certain conditions like Quasi-Steady-State assumption or equilibrium assumption. In any case the mass action law is assumed. For fractional diffusion mass action law does not apply. Thus concentration based models had been upgraded by time depended rate coefficients [1] [13]

2.1 Smoluchowski

2.2 Erban Chapmann

2.3 RevReaddy

3 An Enzymatic Reaction With Fractional Brownian Motion

3.1 Michaelis Menten

3.2 Simulation Model

3.3 Results From Normal Diffusion

3.4 Results from fBm

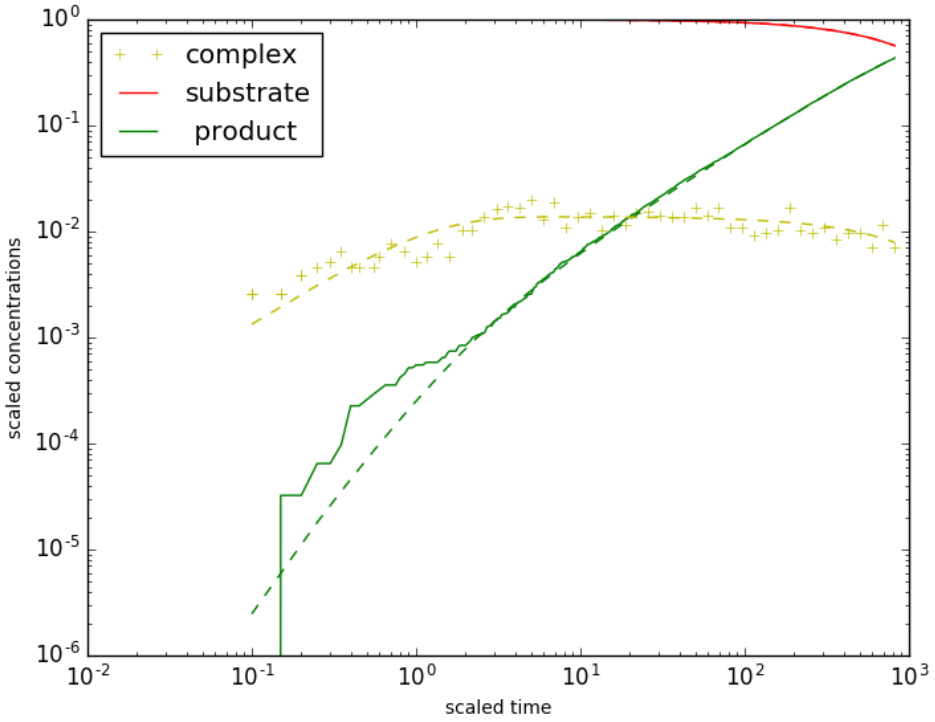

Figure 3.1: Erban Chapmann Concentrations

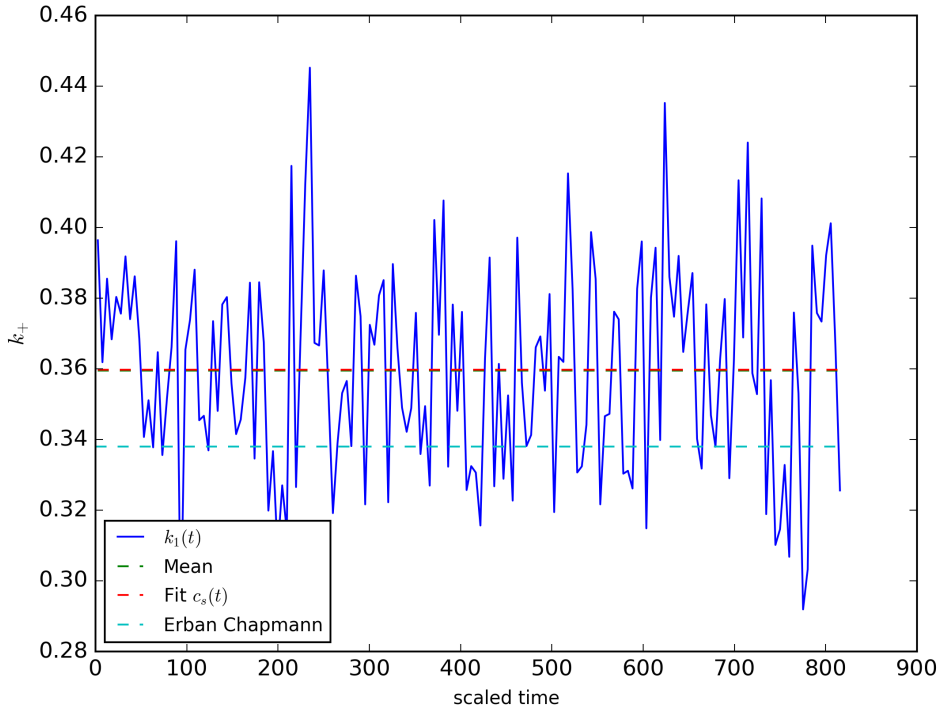

Figure 3.2: Erban Chapmann $k1$

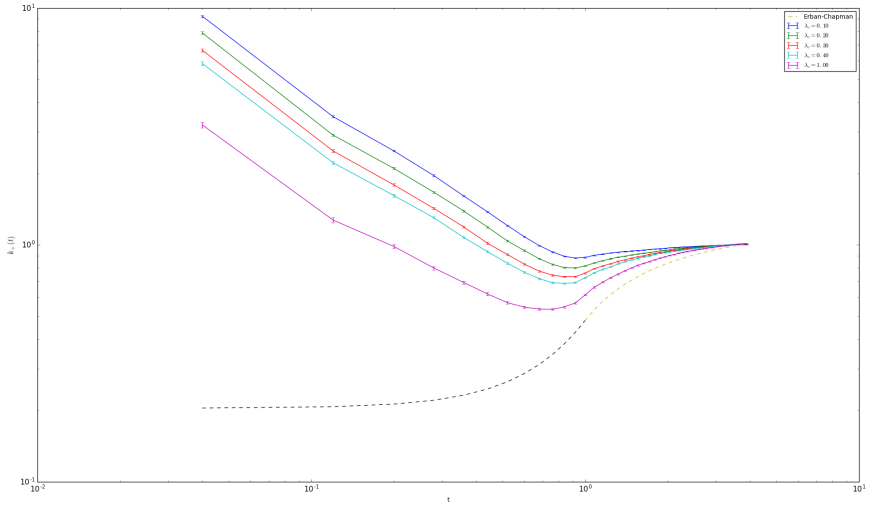

Figure 3.3: Radial distribution for differnt k_c

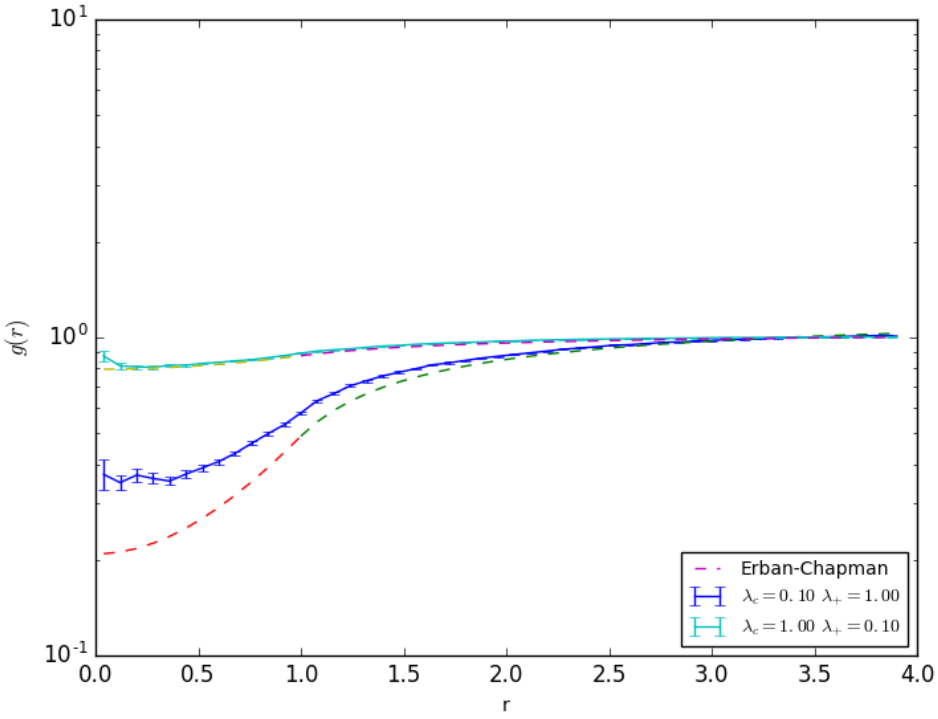

Figure 3.4: Radial distribution for $\lambda_- = 0$

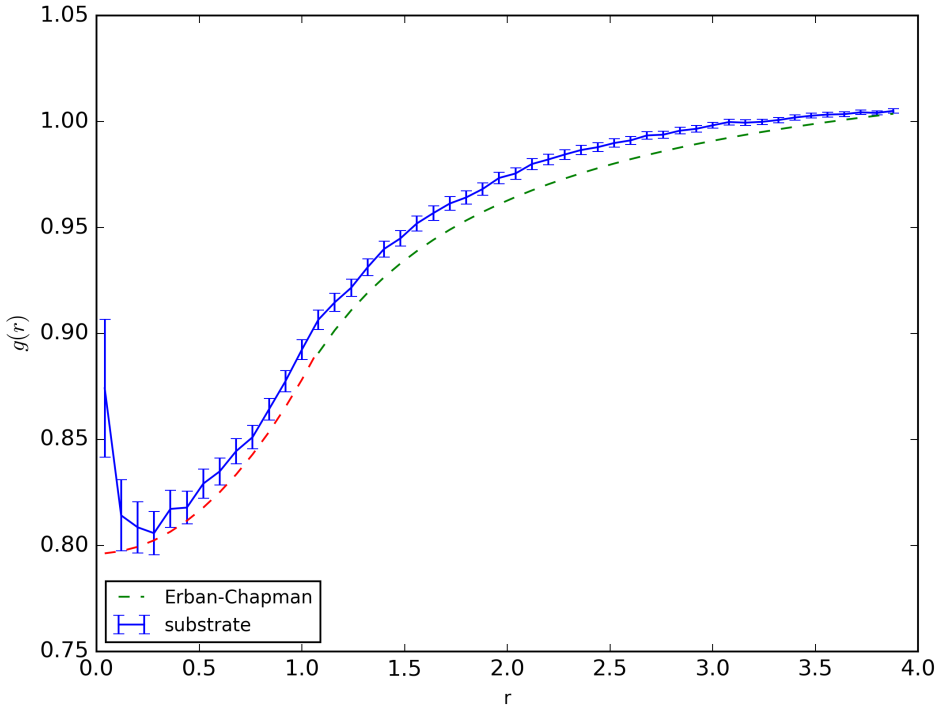

Figure 3.5: Erban Chapmann radial distribution

thesis: $k1(t) \propto t^{-h}$

3.5 Conclusion

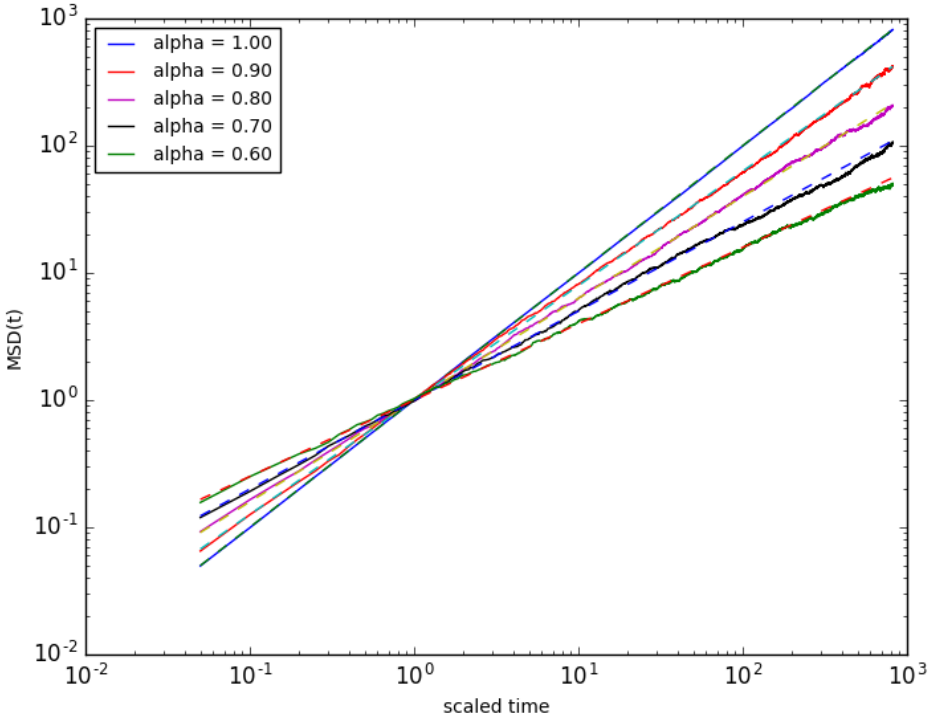

Figure 3.6: different alpha

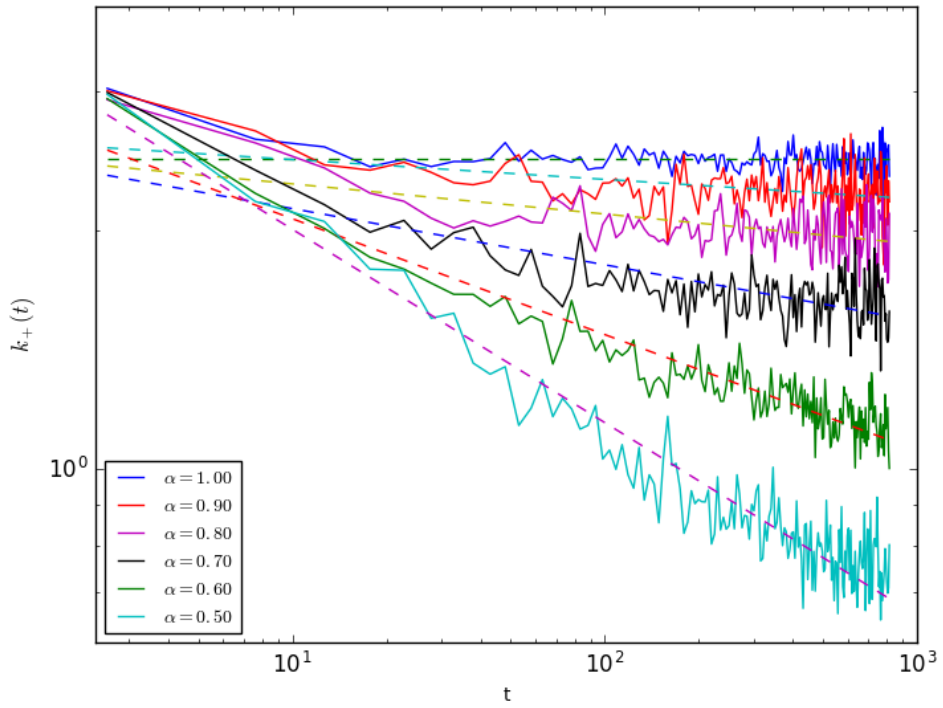

Figure 3.7: $k1(t)$ for differnt α with fitted h

4 Summary

5 Appendix

5.1 From Central Limit Theorem to Gaussian Distribution

In the following the Central Limit Theorem will be applied to calculated the distribution of Y, $\rho(y)dy = P(y < Y < y + dy)$ in the limit of large N , with Y being defined as the sum of an random variable:

$$Y = \frac{1}{\sqrt{N}} \sum_{j=1}^{N} X_j \tag{5.1}$$

The Generating function for a random variable Y is:

$$G_Y(k) = \langle e^{ikY} \rangle = \int e^{ikY} \rho(y) dy \tag{5.2}$$

eq. (5.1) can be inserted into the generating function, which results in:

$$G_Y(k) = \langle e^{\frac{ik}{\sqrt{N}} \sum_{j=1}^{N} X_j} \rangle$$

$$G_Y(k) = \langle \prod_{j=i}^{N} e^{\frac{ik}{\sqrt{N}} X_j} \rangle$$

If all X_j are independent, then:

$$G_Y(k) = \prod_{j=i}^{N} \langle e^{\frac{ik}{\sqrt{N}} X_j} \rangle = e^{\sum_{j=1}^{N} A_j(\frac{k}{\sqrt{N}})} \tag{5.3}$$

$$\text{with } A_j(\frac{k}{\sqrt{N}}) = ln\langle e^{\frac{ik}{\sqrt{N}} X_j} \rangle$$

For large N behavior, we assume $\frac{k}{\sqrt{N}} << 1$ and expand

$$A_j(\frac{k}{\sqrt{N}}) = ln(1 + \langle X_j \rangle \frac{ik}{\sqrt{N}} - \langle X_j^2 \rangle \frac{k^2}{2N} + \mathcal{O}(N^{-\frac{3}{2}})) \tag{5.4}$$

with a finite variance $\sigma_i^2 = \langle X_i^2 \rangle$ and the mean $\langle X_i \rangle = 0$

$$A_j(\frac{k}{\sqrt{N}}) = -\sigma_j^2 \frac{k^2}{2N} + \mathcal{O}(N^{-\frac{3}{2}})) \tag{5.5}$$

Thus, the generating function for large N is:

$$G_Y(k) = e^{-\frac{\sigma^2 k^2}{2}} \tag{5.6}$$
$$\text{with } \sigma = \frac{1}{N}\sum_{j=1}^{N}\sigma_j^2$$

The distribution of Y can be calculated via the inverse Fourier Transform:

$$\rho(y) = \frac{1}{2\pi}\int_{-\infty}^{\infty} e^{-\frac{\sigma^2 k^2}{2}} e^{iky} dk \tag{5.7}$$
$$= \frac{1}{\sqrt{2\pi}\sigma} e^{-\frac{y^2}{2\sigma^2}} \tag{5.8}$$

$\rho(y)$ results in a Gaussian distribution.

5.2 From Gaussian Distribution to Gaussian Transition Probability

The conditional distribution function to be in x at time t if visited position y at time s can be written due to Bayes' theorem as a transition probability from y to x in time $t - s$ multiplied with the probability to be in y at time s:

$$\rho_{t,s}(x, y) = T_{t-s}(x|y)\rho_s(y) \tag{5.9}$$

Further due to particle conservation another relation holds:

$$\rho_t(x) = \int \rho_{t,s}(x, y) dy \tag{5.10}$$

Having an initial condition $\rho_s(x) = \delta(x - y)$:

$$\rho_{t,s}(x|y) = \int \rho_{t,s}(x, y) dy = \int T_{t-s}(x|y)\rho_s(y) dy \tag{5.11}$$
$$= \int T_{t-s}(x|y)\delta(x - y) dy = T_{t-s}(x|y) \tag{5.12}$$

5.3 Einstein Formula

The derivative of the mean variance of the Gaussian distribution in respect to time is defined as:

$$\frac{d}{dt}\delta\boldsymbol{r}^2(t) = \frac{d}{dt}\langle\Delta\boldsymbol{R}^2(t)\rangle = \frac{d}{dt}\int d\boldsymbol{r}\boldsymbol{r}^2 c(\boldsymbol{r}, t) = \int d\boldsymbol{r}\boldsymbol{r}^2 \frac{\partial}{\partial t} c(\boldsymbol{r}, t) \tag{5.13}$$

Fick's second law can be applied:

$$= D \int_{-\infty}^{\infty} d\boldsymbol{r} \boldsymbol{r}^2 \Delta c(\boldsymbol{r}, t) \tag{5.14}$$

Assuming a reasonable assumption $c(\pm\infty, t) = 0$ and two times partial integration one can derive:

$$= -2D \int_{-\infty}^{\infty} d\boldsymbol{r} \boldsymbol{r} \nabla c(\boldsymbol{r}, t) \tag{5.15}$$

$$= 2Dd \int_{-\infty}^{\infty} d\boldsymbol{r} c(\boldsymbol{r}, t) = 2dD \tag{5.16}$$

For the initial condition $\boldsymbol{r}(0) = 0$, one gets the Einstein Formula: $\langle (\boldsymbol{r}(t) - \boldsymbol{r}(0))^2) \rangle = 2dDt$

5.4 Autocorrelation Function for fBm

Subsequently, the VACF in the frequency domain for Fractional Brownian motion can be calculated. The MSD is $\delta r^2(t) =< \Delta R(t) >= 2dK_\alpha t^\alpha$ with K_α being the generalized diffusion-coefficient:

$$\begin{aligned} \tilde{Z}(z) &= \int_0^\infty dt e^{izt} Z(t) \\ &= \frac{1}{2d} \int_0^\infty dt e^{izt} \left[\frac{d^2}{dt^2} \delta r^2(t) \right] \end{aligned}$$

Partial integration:

$$\overset{par.integ.}{=} \frac{1}{2d} \left(\underbrace{\left[e^{izt} \overbrace{\frac{d}{dt} 2dK_\alpha t^\alpha}^{=A(t)} \right]_0^\infty}_{\overset{\alpha \leq 2}{=} 0} - iz \int_0^\infty dt e^{izt} \left[\frac{d}{dt} \delta r^2(t) \right] \right)$$

$$A(t) = \frac{d}{dt} \overbrace{\left[\frac{2dK_\alpha t^{\alpha-1}}{\alpha} \right]}^{B(t)} = \frac{2dK_\alpha t^{\alpha-2}}{\alpha + (\alpha - 1)}$$

Partial integration and Tauber theorem:

$$\tilde{Z}(z) \overset{par.integ.}{=} -\frac{1}{2d}\left(\underbrace{\left[e^{izt}\overbrace{2dK_\alpha t^\alpha}^{=B(t)}\right]_0^\infty}_{\overset{\alpha\leq 1}{=}0} - (iz)^2\int_0^\infty dt e^{izt}\delta r^2(t)\right)$$
$$= -\frac{z^2}{2d}\int_0^\infty dt e^{izt}\delta r^2(t) \overset{\mathrm{Im}(z)>0}{=} K_\alpha\Gamma(1+\alpha)(iz)^{1-\alpha}$$

5.5 Kinetics of the Bi-Molecular Chemical Reaction in Solution

The aim of this calculation is to derive the kinetics for the following reaction scheme:
$\mathrm{A} + \mathrm{B} \underset{k_\mathrm{d}^-}{\overset{k_\mathrm{d}^+}{\rightleftharpoons}} \mathrm{AB}$
The derivation is calculated under the assumption of free diffusion of particle A and B with the diffusion constants D_A and D_B , respectively and without any interactions between them. The joint concentration field can be described by the Smoluchowski equation for a bi-molecular system in a solution:

$$\frac{\partial\rho_t(\boldsymbol{r}_A,\boldsymbol{r}_B)}{\partial t} = (D_A\nabla_A^2 + D_B\nabla_B^2)\rho_t(\boldsymbol{r}_A,\boldsymbol{r}_B) \tag{5.17}$$

The complexity of the problem can be reduced by substituting the positions of the particles A and B with their relative distance $\boldsymbol{r} = \boldsymbol{r}_A - \boldsymbol{r}_B$. It is convenient to introduce even further substitutions:

$$D = D_A + D_B \qquad \boldsymbol{R} = \frac{D_B\boldsymbol{r}_A + D_A\boldsymbol{r}_B}{D_A + D_B} \tag{5.18}$$

the Laplace operator in terms of new coordinates result in:

$$\nabla_A^2 = \left(\nabla_r + \frac{D_B}{D}\nabla_R\right)^2 \tag{5.19}$$

$$\nabla_B^2 = \left(\nabla_r + \frac{D_A}{D}\nabla_R\right)^2 \tag{5.20}$$

Inserting these in eq. (5.17) one gets:

$$\frac{\partial\tilde{\rho}_t(\boldsymbol{r},\boldsymbol{R})}{\partial t} = \left(D\nabla_r^2 + \frac{D_BD_A}{D_A+D_B}\nabla_R^2\right)\tilde{\rho}_t(\boldsymbol{r},\boldsymbol{R}) \tag{5.21}$$

The equation is describing two independent diffusion processes, one in the coordinate $\boldsymbol{r}$ and one in the coordinate $\boldsymbol{R}$. The solution can be obtained by the product ansatz

$\tilde{\rho}_t(\boldsymbol{r}, \boldsymbol{R}) = \rho_t(\boldsymbol{r})q_t(\boldsymbol{R})$. Integration over $\boldsymbol{R}$ results in:

$$\frac{\partial \rho_t(\boldsymbol{r})}{\partial t} = D\nabla_r^2 \rho_t(\boldsymbol{r}) + \frac{D_B D_A}{D_A + D_B} \nabla_R^2 \rho_t(\boldsymbol{r}) \int_{\partial V} q_t(\boldsymbol{R}) d\boldsymbol{a} \tag{5.22}$$

In the previous equation the stokes theorem was applied. The second term is zero due to conservation of probability. The problem is isotropic, hence $r = |\boldsymbol{r}|$ and $\nabla_{\boldsymbol{r}}^2 = \left(\partial_r + \frac{2}{r}\right)\partial$. The equation reduce to one dimension:

$$\frac{\partial \rho_t(r)}{\partial t} = -\left(\frac{\partial}{\partial_r} + \frac{2}{r}\right) j_t(r) \qquad j_t(r) = D\frac{\partial \rho_t(r)}{\partial_r} \tag{5.23}$$

The stationary distribution results in:

$$0 = -\left(\frac{\partial}{\partial_r} + \frac{2}{r}\right) j_t^s(r) \tag{5.24}$$

$$\frac{dj_t^s(r)}{j_t^s(r)} = -\frac{2}{r}dr \tag{5.25}$$

$$j_t^s(r) = Ar^{-2} \tag{5.26}$$

$$\rho^s(r) = \rho^s(r_0) - \frac{\int_{r_0}^r j_t^s(r')dr'}{D} = \rho^s(r_0) + \frac{A}{D}\left(\frac{1}{r} - \frac{1}{r_0}\right) \tag{5.27}$$

Now assuming only a single B molecule being at the position $r = 0$. Instantaneous reaction occur for $r \leq \sigma \Rightarrow \rho_t(r \leq \sigma) = 0$. For $r \to \infty$ the distribution is than defined as the concentration of particle A $\rho_t(r \to \infty) = c_A$ and the Solutions for $\rho^s(r)$ and $j_t^s(r)$ for the boundary conditions are:

$$\rho^s(r) = C_A\left(1 - \frac{\sigma}{r}\right) \qquad j_t^s(r) = -D\sigma C_A r^{-2} \tag{5.28}$$

The change of the concentration of C_{AB} is then:

$$\frac{dC_{AB}}{d} = 4\pi\sigma D C_A C_B \tag{5.29}$$

By formulating the problem in relative distance from particle A and B. It was also reasonable to keep particle B at its initial position. The results shows the relation between the product of the concentrations and the concentration change.In the derivation of Michealis-Menten kinetics this is an assumption.

5.6 Michaelis-Menten Kinetics

Michaelis-Menten kinetics are describing the following system:
$\mathrm{S} + \mathrm{E} \underset{k_1'}{\overset{k_1}{\rightleftarrows}} \mathrm{ES} \xrightarrow{k_2} \mathrm{P} + \mathrm{E}$. A range of differential equations can be formulated as a result of particle conservation and the assumption for a bi-molecular chemical

reaction to be proportional to the product of the reactants concentration.

$$\frac{d[P]}{dt} = k_2[ES] \tag{5.30}$$

$$\frac{d[E]}{dt} = k_2[ES] + k_1'[ES] - k_1'[E][S] \tag{5.31}$$

$$\frac{d[S]}{dt} = k_1'[ES] - k_1'[E][S] \tag{5.32}$$

$$\frac{d[ES]}{dt} = -k_2[ES] - k_1'[ES] + k_1'[E][S] \tag{5.33}$$

With a quasi-steady-state approximation: $\frac{d[ES]}{dt} = 0 \longrightarrow k_1[E][S] = k_1'[ES]+k_2[ES]$. A Rearrangement of this equation results in the Michaelis-Menten constant: $K_M = \frac{k_1'+k_2}{k_1} = \frac{[E][S]}{[ES]}$. From the enzyme conservation law one gets:

$$[E] = [E]_0 - [ES] \tag{5.34}$$

After inserting eq. (5.34) into the quasi-steady-state approximation, one gets:

$$[ES] = \frac{[E]_0[S]}{K_M + [S]} \tag{5.35}$$

Combining it with the first differential eq. (5.31) one gets the rate of Product production:

$$v = \frac{d[P]}{dt} = k_2\frac{[E]_0[S]}{K_M + [S]} = V_{max}\frac{[S]}{K_M + [S]} \tag{5.36}$$

Bibliography

[1] Hugues Berry.
Monte carlo simulations of enzyme reactions in two dimensions: fractal kinetics and spatial segregation.
Biophysical journal, 83(4):1891–1901, 2002.

[2] Peter F. Craigmile.
Simulating a class of stationary Gaussian processes using the Davies-Harte algorithm, with application to long memory processes.
Journal of Time Series Analysis, 24(5):505–511, 2003.

[3] R. B. DAVIES and D. S. HARTE.
Tests for hurst effect.
Biometrika, 74(1):95–101, 1987.

[4] Höfling Felix.
Stochastic processes and correlation functions.
University Lecture, 2016.

[5] Felix Höfling and Thomas Franosch.
Anomalous transport in the crowded world of biological cells.
Reports on Progress in Physics, 76(4):046602, apr 2013.

[6] Peter Horvai, Tomasz Komorowski, and Jan Wehr.
Finite time approach to equilibrium in a fractional brownian velocity field.
Journal of Statistical Physics, 127(3):553–565, feb 2007.

[7] J. R. M. Hosking.
Modeling persistence in hydrological time series using fractional differencing.
Water Resources Research, 20(12):1898–1908, 1984.

[8] Steven B. Lowen.
Efficent generation of fractional brownian motion for simulation of infrared focal-plane array calibration drift.
Methodology And Computing In Applied Probability, 1(4):445–456, 1999.

[9] Benoit B. Mandelbrot and John W. Van Ness.
Fractional Brownian Motions, Fractional Noises and Applications.
SIAM Review, 10(4):422–437, oct 1968.

[10] Leonor Michaelis and Maud L Menten.
Die kinetik der invertinwirkung.
Biochem. z, 49(333-369):352, 1913.

[11] Allen P Minton.
How can biochemical reactions within cells differ from those in test tubes?

Journal of cell science, 119(Pt 14):2863–9, 2006.

[12] Hong Qian.
Fractional brownian motion and fractional gaussian noise.
In *Processes with Long-Range Correlations*, pages 22–33. Springer, 2003.

[13] S Schnell and TE Turner.
Reaction kinetics in intracellular environments with macromolecular crowding: simulations and rate laws.
Progress in biophysics and molecular biology, 85(2):235–260, 2004.

[14] M. Timmer, J.;Koenig.
On generating power law noise.
Astronomy and Astrophysics, 300(1):707, 1995.

[15] Dieker Ton.
Simulation of fractional brownian motion.
Master's thesis, 2004.